The V0-ATPase mediates apical secretion of exosomes containing Hedgehog-related proteins in *Caenorhabditis elegans*

Samuel Liégeois, Alexandre Benedetto, Jean-Marie Garnier, Yannick Schwab, and Michel Labouesse

Institut de Génétique et de Biologie Moléculaire et Cellulaire, Centre National de la Recherche Scientifique, Institut National de la Santé et de la Recherche Médicale, Universite Louis Pasteur, 67400 Illkirch, France

Polarized intracellular trafficking in epithelia is critical in development, immunity, and physiology to deliver morphogens, defensins, or ion pumps to the appropriate membrane domain. The mechanisms that control apical trafficking remain poorly defined. Using *Caenorhabditis elegans*, we characterize a novel apical secretion pathway involving multivesicularbodies and the release of exosomes at the apical plasma membrane. By means of two different genetic approaches, we show that the membrane-bound V0 sector of the vacuolar H^+-ATPase (V-ATPase) acts in this pathway, independent of its contribution to the V-ATPase proton pump activity. Specifically, we identified mutations in the V0 "a" subunit VHA-5 that affect either the V0-specific function or the V0+V1 function of the V-ATPase. These mutations allowed us to establish that the V0 sector mediates secretion of Hedgehog-related proteins. Our data raise the possibility that the V0 sector mediates exosome and morphogen release in mammals.

Introduction

All developmental and physiological functions performed by epithelia depend on the polarized targeting of the plasma membrane and secreted proteins to either the apical or basolateral plasma membranes (Rodriguez-Boulan et al., 2005). Cargo proteins sorted in the Golgi apparatus and the endosomal system through sets of basolateral- and apical-specific sorting determinants are transported to the plasma membrane following partially different routes (Hoekstra et al., 2004; Rodriguez-Boulan et al., 2005). Although basolateral secretion has been fairly well characterized, the mechanisms involved in apical trafficking remain poorly defined (Rodriguez-Boulan et al., 2005).

Basolateral sorting signals usually correspond to tyrosine or dileucine residues found in the COOH terminus of proteins. They are recognized by basolateral-specific adaptor complexes (Bonifacino and Lippincott-Schwartz, 2003; Rodriguez-Boulan et al., 2005), such as AP-1B in epithelial cells (Folsch et al., 1999). Before membrane fusion and SNARE action, vesicles are thought to be tethered to the basolateral membrane by the exocyst complex (Whyte and Munro, 2002), which was initially identified in yeast (TerBush and Novick, 1995). In metazoans, the exocyst is required for basolateral delivery of the LDL receptor in MDCK cells (Grindstaff et al., 1998; Yeaman et al., 2001), of E-cadherin in the *Drosophila melanogaster* notum (Langevin et al., 2005), and for Rhodopsin1 transport in *D. melanogaster* photoreceptor cells (Beronja et al., 2005). Recent results suggest that AP-1B and the exocyst act primarily in recycling endosomes (Ang et al., 2004; Beronja et al., 2005; Langevin et al., 2005; Lock and Stow, 2005; Satoh et al., 2005), which underlines the central role of this organelle in sorting processes. Indeed, recycling endosomes may be compartmentalized into apical- and basolateral-related domains, or even divided into distinct organelles, suggesting that they could also play a critical role in apical trafficking (Hoekstra et al., 2004; Rodriguez-Boulan et al., 2005).

Aside from this possible role of recycling endosomes, all other aspects of sorting along the basolateral and apical routes seem to differ. Apical signals are more diverse and often correspond to posttranslational adducts, such as lipids or glycans (Schuck and Simons, 2004; Rodriguez-Boulan et al., 2005). For instance, the Hedgehog morphogen is secreted apically upon

S. Liégeois and A. Benedetto contributed equally to this paper.

Correspondence to Michel Labouesse: lmichel@igbmc.u-strasbg.fr

S. Liégeois's present address is Institut de Biologie Moléculaire et Cellulaire, F-67000 Strasbourg, France.

Abbreviations used in this paper: DIC, differential interference contrast; mRFP, monomeric red fluorescent protein; MVB, multivesicular body; SEM, scanning electron microscopy; TEM, transmission electron microscopy; V-ATPase, vacuolar H^+-ATPase.

The online version of this article contains supplemental material.

The Journal of Cell Biology, Vol. 173, No. 6, June 19, 2006 949–961
http://www.jcb.org/cgi/doi/10.1083/jcb.200511072

cholesterol addition, but basolaterally otherwise (Gallet et al., 2003). No specific apical cytosolic complex, akin to AP-1B or the exocyst, has been identified so far. Instead, protein clustering, possibly through lipid rafts, is thought to mediate the sorting and transport of apical cargoes (Schuck and Simons, 2004; Rodriguez-Boulan et al., 2005). In particular, glycosyl phosphatidylinositol–linked proteins appear to form oligomers that are directly targeted to the apical membrane (Paladino et al., 2004, 2006; Hua et al., 2006). Several proteins have been proposed to play an active role in apical protein clustering, raft formation, and/or apical delivery, such as caveolins (Kurzchalia et al., 1992), annexin 13b (Fiedler et al., 1995), and the tetraspan protein VIP17/MAL (Cheong et al., 1999; Puertollano et al., 1999). However, their mechanistic roles have not been fully elucidated, or their implication has been questioned (Manninen et al., 2005). In addition to the limited understanding of apical secretion at the molecular level, it is not clear whether the terminal fusion process involves small vesicles, such as those defined at synapses, or larger organelles, such as secretory lysosomes (Blott and Griffiths, 2002).

Hence, despite the many critical findings originating from tissue culture cells (Rodriguez-Boulan et al., 2005), investigations with other systems and other cargo proteins could help to elucidate the mechanisms involved in apical exocytosis. *Caenorhabditis elegans*, which has contributed to decipher the mechanisms controlling vesicular trafficking (Nurrish, 2002), provides such an in vivo model. We have chosen to analyze apical secretion of cuticle proteins by the epidermis. The cuticle includes glycosylated collagens, glycosyl phosphatidylinositol–linked cuticlins, and lipid-modified Hedgehog-related peptides (McMahon et al., 2003; Sapio et al., 2005; Zugasti et al., 2005). We previously suggested that the gene *che-14* is required for cuticle secretion (Michaux et al., 2000). The CHE-14 protein is the *C. elegans* orthologue of *Drosophila* Dispatched, which participates in apical targeting of cholesterol-modified Hedgehog (Burke et al., 1999; Gallet et al., 2003).

While searching for *che-14* alleles (Michaux et al., 2000), we uncovered several additional mutations inducing *che-14*–like phenotypes and reasoned that they might identify new components of the apical trafficking pathway. Two such mutations, *mc37* and *mc38*, proved to be small deletions behaving as genetic-null alleles of the gene *vha-5* (unpublished data). The gene *vha-5* encodes one of the four *C. elegans* "a" subunits of the V0 sector of the vacuolar H^+-ATPase (V-ATPase), and is required for development beyond the L2 larval stage (Oka et al., 2001; Pujol et al., 2001). The V-ATPase is a multisubunit protein complex consisting of two subcomplexes called the V0 and V1 sectors (Fig. 1 A). The cytosolic V1 sector hydrolyses ATP and provides the energy to pump protons through the transmembrane proteolipid pore formed by the V0 sector (Nishi and Forgac, 2002). The V-ATPase is the main proton pump establishing a pH gradient in the secretory and endocytic pathways. It generates a proton-motive force that is essential to load synaptic vesicles with neurotransmitters before secretion (Amara and Kuhar, 1993). The V-ATPase is also found at the apical plasma membrane of polarized cells, where it is essential for osmoregulation in animal excretory systems (Nishi and Forgac, 2002). More recently, biochemical and genetic data suggested that the V0 sector can play a role independently from the V1 sector. In *Saccharomyces cerevisiae*, vacuoles deficient for the "a" subunit Vph1p do not fuse efficiently (Peters et al., 2001; Bayer et al., 2003). In *D. melanogaster*, neurons lacking the "a" subunit Vha100 accumulate vesicles in synaptic terminals (Hiesinger et al., 2005). In both cases, the defects were independent of the proton gradient and placed downstream of SNARE function (Peters et al., 2001; Bayer et al., 2003; Hiesinger et al., 2005).

By further dissecting the role of *vha-5* using targeted mutagenesis, and by comparing phenotypes resulting from the inactivation of V1 or V0 subunits, we uncover a specific role for the V0 sector in mediating secretion to the apical membrane. In particular, we show that the V0 sector is required for apical secretion of Hedgehog-related peptides through a multivesicular compartment able to release exosomes.

Results

The V0 "a" subunit VHA-5 is apical and required for cuticle formation

To determine the distribution and subcellular localization of VHA-5, we raised polyclonal antibodies against its cytoplasmic NH_2 terminus. In addition, we generated a COOH-terminal VHA-5::GFP fusion, which rescued the larval lethality caused by the *vha-5(mc38)* deletion (Fig. 1 B). The VHA-5 antiserum recognized a 105-kD protein in wild-type extracts (Fig. 1 C, lane a). To prove its specificity, we examined extracts from *vha-5(mc38)* homozygous animals carrying the rescuing VHA-5::GFP construct. The VHA-5 antiserum failed to detect the ~105-kD band in these extracts, but detected an ~135-kD band (Fig. 1 C, lane b). These results are consistent with *vha-5(mc38)* being a small deletion associated with a frameshift (Fig. 1 B and not depicted) and with the presence of 257 additional residues in the GFP-fusion protein. We conclude that the VHA-5 antiserum is specific and that *vha-5(mc38)* is a molecular null mutation.

In agreement with previously published observations (Oka et al., 2001; Pujol et al., 2001), we found that VHA-5 is expressed in the H-shaped excretory cell corresponding to the *C. elegans* kidney-like organ (Fig. 1, D and E). It is also expressed in the main epidermal syncytium (Fig. 1, D–F), which had previously been overlooked. The excretory cell extends long processes called excretory canals where osmoregulation takes place (Nelson and Riddle, 1984), whereas the epidermis controls body length and apical cuticle secretion (White, 1988). VHA-5 colocalized apically with the V1 subunit VHA-8 in both tissues (Fig. 1 E; note that VHA-5 is not expressed in the lateral epidermis). VHA-5 was localized at the level of apical membrane stacks by immunogold staining (Fig. 1 G). Consistent with VHA-5 distribution and a role of the V-ATPase in osmoregulation (Nishi and Forgac, 2002), *vha-5(mc38)* larvae filled with fluid and died at the L1 stage (unpublished data), which corresponds to the phenotype observed after laser ablation of the excretory cell (Nelson and Riddle, 1984). In addition, *vha-5(mc38)* L1 larvae had a severe malformation of the lateral cuticular specializations known as alae (Fig. 1 D and Fig. 2 A), which are primarily synthesized by the lateral seam cells.

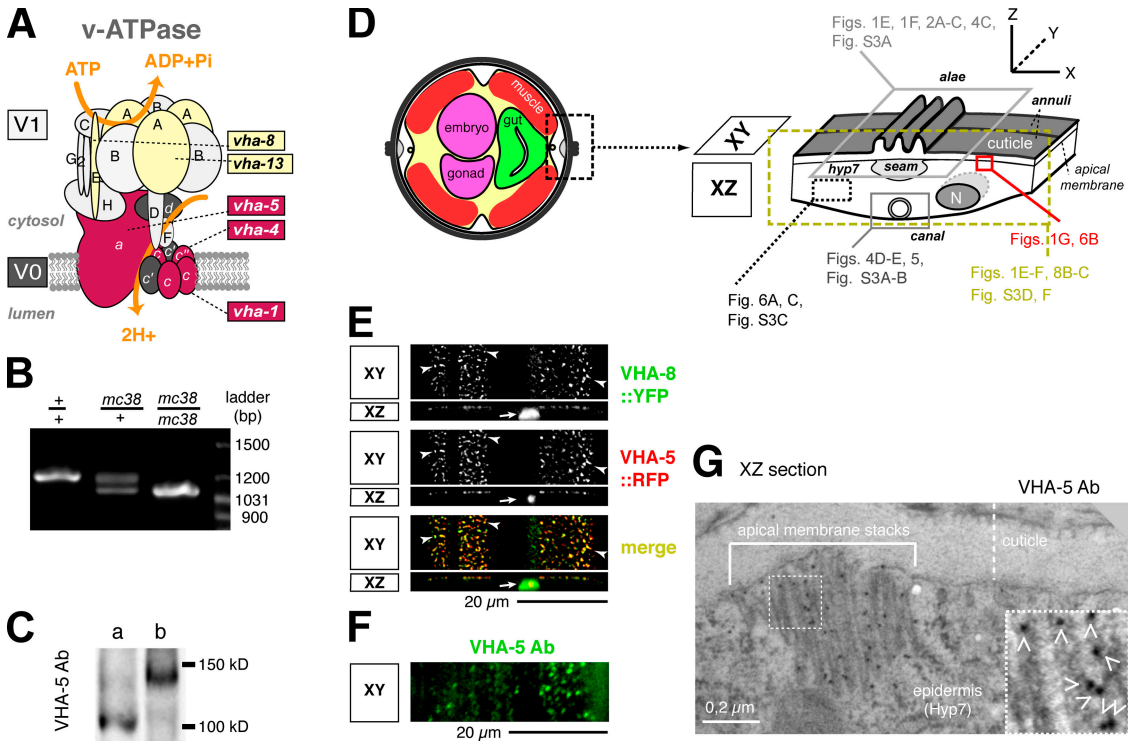

Figure 1. **VHA-5 is at the apical membrane in the excretory canal and the epidermis.** (A) Drawing of the V-ATPase complex and *C. elegans* subunits analyzed in this study. (B) PCR analysis of wild-type, *vha-5(mc38)/+*, and *vha-5(mc38)* animals with primers in *vha-5* showing that *mc38* is a small deletion. (C) Western blot with a VHA-5 antiserum of wild-type *C. elegans* extracts (lane a) and *vha-5(mc38)* mutants rescued by a *vha-5::gfp* transgene (lane b). A 105-kD band is visible in wild-type animals, a 135-kD band in rescued *vha-5(mc38)* mutants. (D) Drawing of a section through the body (left) and the epidermis (right) showing the positions of the images displayed in this and other figures. (E) Distribution of *vha-5::rfp* and *vha-8::yfp* in rescued *vha-5(mc38)* animals; XY confocal section, apical epidermal surface where the pattern appears as dots (arrowheads; excretory canal, arrows). The V1 E subunit VHA-8 (see A) colocalizes with VHA-5. (F) Immunofluorescence image of a wild-type adult with VHA-5 antiserum; VHA-5 forms dots in the epidermis. (G) Immunogold labeling against VHA-5 (gold beads, arrowheads); VHA-5 localizes mainly to apical membrane stacks of the epidermis (see also Fig. S5 D). Fig. S5 is available at http://www.jcb.org/cgi/content/full/jcb.200511072/DC1.

Although VHA-5 is not expressed in these cells, the main epidermal syncytium also contributes to their morphogenesis (Sapio et al., 2005). Because VHA-5 is transmembraneous and not cuticular, the simplest interpretation for this phenotype is that *vha-5* mutations compromise the secretion of proteins needed for alae formation.

The V0 sector alone is required for cuticle formation

As outlined in the previous section, the V0 sector may fulfill two distinct functions; either working together with the V1 sector to mediate proton pumping or working alone, as in yeast and *D. melanogaster* neurons, to mediate membrane fusion. To determine which of these functions could account for the cuticle secretion defect observed in *vha-5(mc38)* larvae, we examined the role of other V-ATPase subunits in cuticle formation using the RNAi approach. If improper proton pumping is responsible for the aforementioned *vha-5* cuticle defects, RNAi knockdown of either V0 or V1 subunits should result in similar cuticular defects. Conversely if the loss of a V0-specific function accounts for the *vha-5* cuticular phenotype, only RNAi knockdown of V0 subunits should phenocopy *vha-5* cuticle defects. We chose two V1 subunits (VHA-8 and -13) and one V0 subunit (VHA-4) encoded by single-copy genes, which were, thus, expected to be ubiquitously expressed and to display RNAi phenotypes of comparable severity. In addition, we tested RNAi against the three genes encoding the V0 "c" subunit (*vha-1*, *-2*, and *-3*), which are >78% identical at the nucleotide level. We found that the RNAi phenotype of *vha-1* was the strongest and was directly comparable to that of *vha-4*, *-8,* and *-13* (Fig. 2 B'), presumably because it reflects knockdown of all three paralogs.

RNAi against these V1 or V0 subunit genes led to 100% lethality in the progeny of treated animals (Fig. 2 B', bottom bars). It is likely that most embryos died because of a defect in yolk endocytosis, which is known to be sensitive to proton pumping (Choi et al., 2003). In agreement, we found that yolk vitellogenin-GFP accumulated in the pseudocoelom of RNAi-treated animals rather than in oocytes and embryos (Fig. S1, available at http://www.jcb.org/cgi/content/full/jcb.200511072/DC1). Despite the strong lethality induced by loss of V-ATPase function, a few L1 larvae hatched and, invariably, died filled with fluid before the L2 larval stage (Fig. 2 B"), as observed for *vha-5(mc38)* larvae. Strikingly, we observed before their death that L1 hatchlings displayed severe alae defects when RNAi targeted the V0 subunits *vha-1* or *-4*, but had wild-type alae after knockdown of the V1 subunits *vha-8* or *-13* (Fig. 2, B and B'). Consistent with the phenotype of *vha-5*–null mutants, RNAi against *vha-5* also affected alae formation (Fig. 2, B and B'–C),

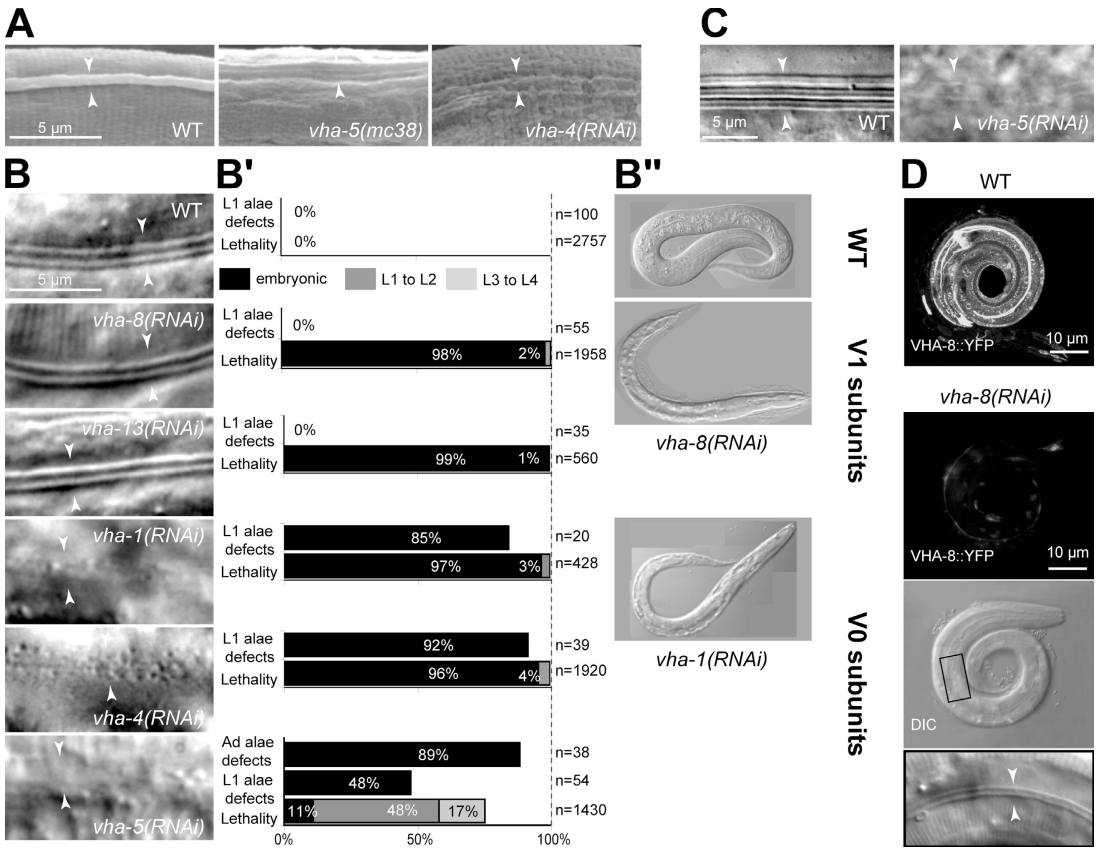

Figure 2. **The V0 sector is specifically required for cuticle secretion.** (A) Alae (arrowheads) of wild-type (WT), *vha-5(mc38)*, and *vha-4(RNAi)* L1 larvae visualized by SEM; *vha-5(mc38)* and *vha-4(RNAi)* larvae have essentially no alae. (B–B″) Alae (arrowheads; B), quantification of lethality and alae defects (B′) and a representative larva filled with fluid (B″) after RNAi knockdown of the V1 subunits VHA-8 and -13, or V0 subunits VHA-1, -4, and -5; images (in B and B″) correspond to DIC micrographs. Lethality, and L1 or adult (Ad) alae defects, were quantified in separate experiments. (C) Alae (arrowheads) of a wild-type adult and an animal that survived until adulthood after RNAi against *vha-5*. Alae are absent in the VHA-5–defective adult. (D) GFP fluorescence of a control L1 larva carrying a *vha-8::gfp* transgene (WT), and after RNAi against *vha-8* (*vha-8(RNAi)*). The RNAi treatment almost completely removed the fluorescence in this larva, yet it has normal alae (see magnified view of the boxed area in the bottom DIC image).

although lethality was weaker because VHA-5 is not ubiquitously expressed like VHA-4. One trivial explanation for the persistence of normal alae after V1 subunit knockdown could be that RNAi was less efficient than for V0 subunits. It is unlikely, as the lethality rates and the larval osmoregulation defects observed after V1 and V0 subunit knockdown were comparable (Fig. 2, B' and B"), hinting that both RNAi were equally effective. To support this idea, we submitted a *vha-8::gfp* transgenic strain to *vha-8* RNAi and verified that it induced a drastic decrease of VHA-8::GFP fluorescence (Fig. 2 D). We conclude that the V0 sector is required independently from the V1 sector for apical secretion of some cuticle components.

The two functions of V0 are genetically separable

If the V0 sector has two distinct functions, it should be possible to recover *vha-5* alleles that affect either its V0-specific secretion function or its V0+V1 proton-pump function. The *vha-5* distribution and the aforementioned phenotypes indicate that reducing V0-specific function should affect cuticle secretion, whereas impairing proton pumping should affect the excretory canal responsible for osmoregulation. To identify such mutations, we used a plasmid rescue strategy, whereby we generated mutations by using PCR on a rescuing *vha-5::gfp* construct, introducing them into *vha-5(mc38)/+* animals, and recovering live homozygous *vha-5(mc38)* animals whenever possible (Fig. 3 A). We modified charged or large hydrophobic residues, as well as residues previously mutated in the yeast Vph1p (Leng et al., 1996, 1998). We generated 56 mutations (Fig. 3, B and C; and Fig. S2, available at http://www.jcb.org/cgi/content/full/jcb.200511072/DC1); 42 had no obvious phenotype by differential interference contrast (DIC) microscopy (Fig. 3 B, stars), and eight failed to rescue, indicating that those residues are essential for VHA-5 function (Fig. 3 B, white boxes). More interestingly, six substitutions rescued the *vha-5(mc38)*–induced lethality and affected the cuticle, the excretory canal, or both.

These six mutations defined three classes, which we will call "cuticle mutations" (L786S, E830Q, and V844F), "canal mutations" (W190A and R191A), or "mixed mutations" (W327A). First, animals carrying cuticle or mixed mutations were significantly shorter and dumpier than wild-type animals or animals carrying canal mutations (Fig. 4 A). This phenotype is frequently observed for mutations affecting cuticle components (McMahon et al., 2003). Western blot analysis using the VHA-5 antiserum detected similar amounts of mutant VHA-5::GFP proteins (Fig. 4 B), implying that expression level

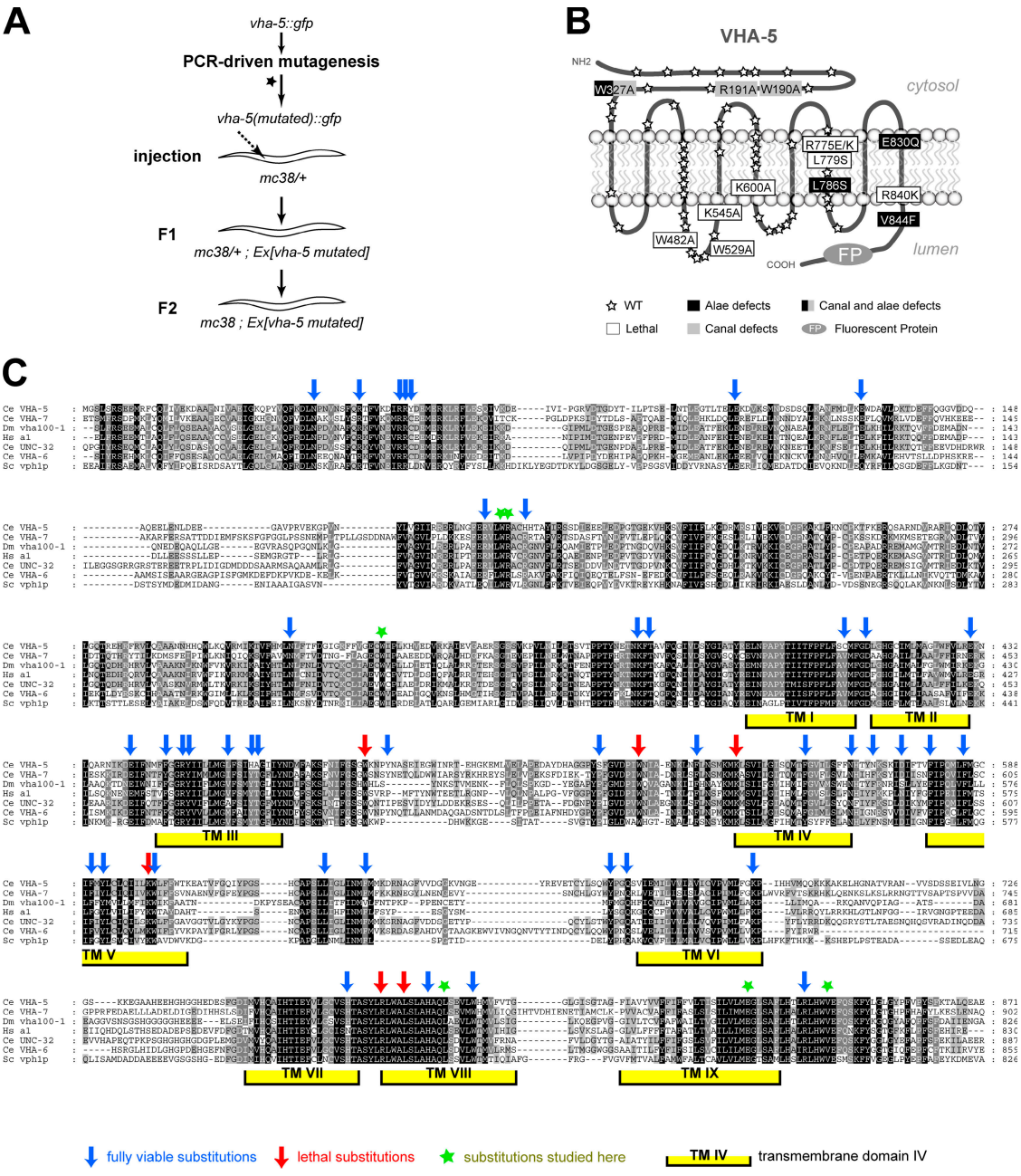

Figure 3. **Mutations introduced in the V0 subunit VHA-5.** (A) Strategy to generate *vha-5* mutations based on complementation of the *vha-5*–null allele *vha-5(mc38)*. (B) Predicted topology for VHA-5 based on yeast Vph1p (Nishi and Forgac, 2002) and positions of substitutions. Box, symbols for the most important phenotypes (see also Fig. S2). DbClustal alignment (http://bips.u-strasbg.fr/PipeAlign/jump_to.cgi?DbClustal+noid) of VHA-5 with the three other *C. elegans* "a" subunits, VHA-6 (intestinal), VHA-7 (epidermal), and UNC-32 (ubiquitous in the embryo, and then muscular and neuronal), the most closely related human and fly "a" subunits (human ATP6V0a1 and *D. melanogaster* V100), and the *S. cerevisiae* "a" subunit Vph1p. The positions of the mutations and the predicted positions of the transmembrane domains (numbered with roman letters) are indicated above VHA-5. Fig. S2 is available at http://www.jcb.org/cgi/content/full/jcb.200511072/DC1.

differences do not explain phenotypic differences. Second, scanning electron microscopy (SEM) showed that adult alae were strongly affected in the former, but not the latter, animals (Fig. 4 C and Fig. S3 A, available at http://www.jcb.org/cgi/content/full/jcb.200511072/DC1). Third, confocal microscopy using the mutant VHA-5::GFP as a marker and transmission electron microscopy (TEM) revealed that the excretory canal of animals with canal or mixed mutations, but not with cuticle mutations, was abnormal (Fig. 4, D and E; and Fig. S3, A and B). Their excretory canals had an increased section, often with multiple lumens, and 3–10 abnormal whorls per canal (see *mc38; Ex[W190A]* in Fig. 4 [D and E]). Strikingly, we observed similar phenotypes by knocking down V1 or V0 subunits by RNAi from L3 larval stage until adulthood (Fig. 5). Thus, we infer that the defects induced by canal mutations reflect an impairment of V0+V1 proton pumping, and that they are caused by loss-of-function rather than by gain-of-function mutations. Expansion of the excretory canal in these mutants might help

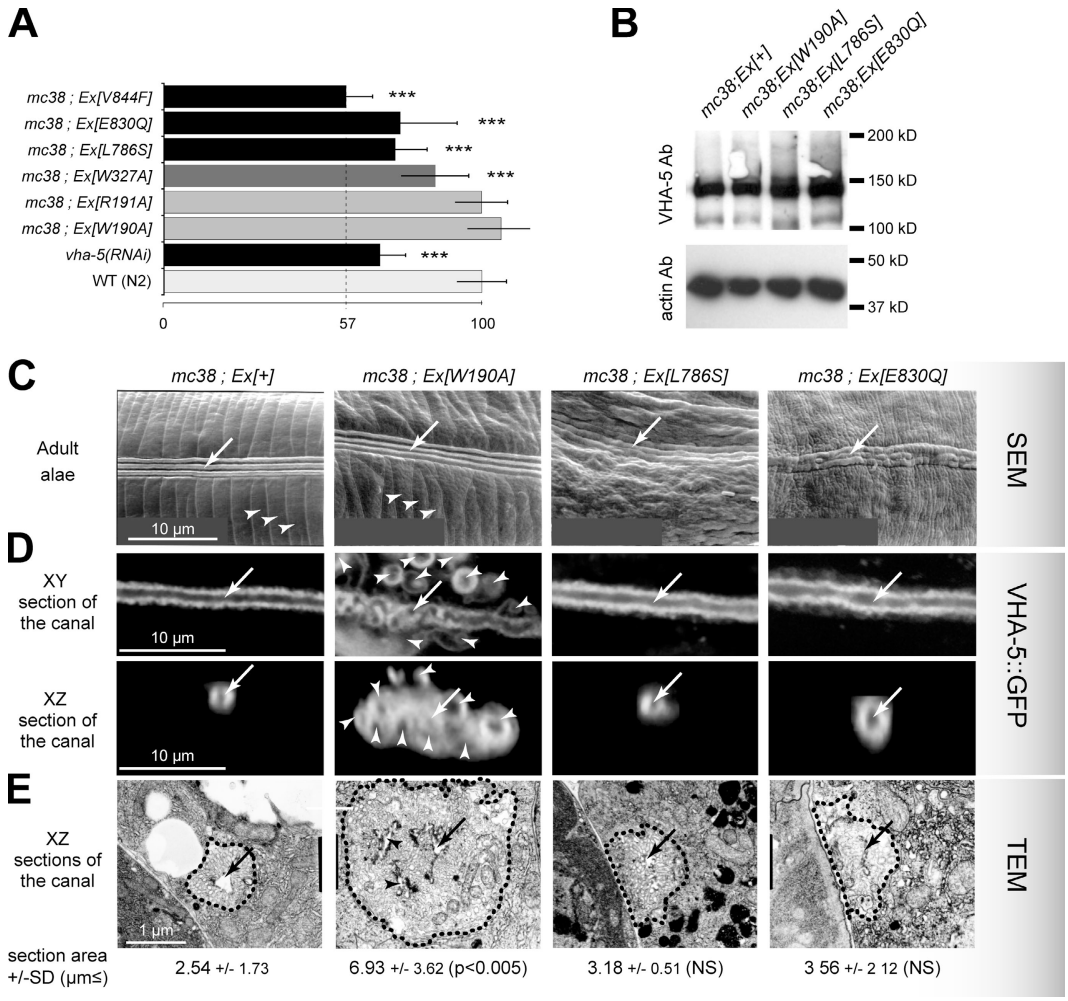

Figure 4. **Genetic separation of the V0-specific and V0+V1 functions of the V0 subunit VHA-5.** (A) Body length of adults at the same age (Error bars represent the SD; ***, significantly different from wild-type with $P < 0.0001$). In this and subsequent figures, *vha-5(mc38)* animals with a mutant *vha-5::gfp* or *vha-5::rfp* transgenic are noted *mc38; Ex[substitution]*. (B) Western blot analysis with VHA-5 antiserum of extracts prepared from the three main mutants described in the text. The VHA-5::GFP protein levels are comparable, relative to an actin loading control. (C) Adult outer cuticle, alae (arrows), and annuli (arrowheads) observed by SEM (genotypes indicated above images). Note the stunted alae and annuli defects induced by L786S and E830Q mutations. (D) GFP fluorescence of the VHA-5 construct in the excretory canal of similar adults (top row, single XY confocal section; bottom row, transverse XZ projection. Compare the normal lumen (arrow) in the control animal with the whorls (arrowheads) induced by the W190A mutation. (E) Excretory canal in similar adults observed by TEM, and quantification of the canal section area. Note the multiple lumens (black arrowheads) in *mc38; Ex[W190A]* animals (dotted lines outline the excretory canal). NS, not significantly different from control animals; SD, standard deviation.

to compensate for the decrease in proton-pumping efficiency. Surprisingly, animals with canal mutations did not show any proton-pumping defect in the epidermis. Possibly, proton pumping is preserved in this tissue because the "a" subunit VHA-7, which is expressed in the epidermis but not in the excretory cell (Oka et al., 2001; Pujol et al., 2001), compensates for the mutated VHA-5. In contrast, we infer that the cuticle defects induced by cuticle mutations reflect an impairment of the V0-specific secretion function, which would not be compensated by other "a" subunits, probably because they are not endowed with this specific function. The existence of various "a" subunits with possibly different functions in the epidermis is reminiscent of the difference observed in yeast between Vph1p and Stv1p (Kawasaki-Nishi et al., 2001). Lastly, we suggest that the mixed mutation W327A affects both V0+V1 and V0-specific functions. We note that cuticle mutations are located in the last

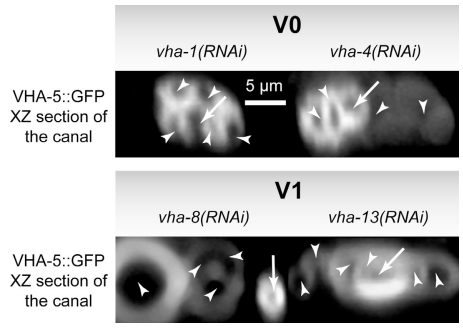

Figure 5. **Knockdown of V0 and V1 subunits induces whorls in the excretory canal.** VHA-5::GFP fluorescence in the excretory canal of adults after RNAi against V0 (*vha-1* and *vha-4*) or V1 (*vha-8* and *vha-13*) subunits performed during larval development. Note the presence of whorls (arrowheads; the normal lumen is outlined with arrows), as in *mc38; Ex[W190A]* animals (Fig. 4 D).

transmembrane domain or in the COOH-terminal luminal tail, whereas canal mutations are in the NH_2-terminal cytoplasmic part, which is more likely to interact with the V1 sector (Nishi and Forgac, 2002). We conclude that the V0-specific and V0+V1 functions of VHA-5 are genetically separable.

V0 mediates secretion of exosomes through MVBs

If indeed the V0 sector is involved in secretion, *vha-5* cuticle mutants should accumulate secretory organelles. At low magnification, TEM through the epidermis showed that animals carrying cuticle or mixed mutations contained significantly more and larger dense organelles than wild-type adults or animals carrying canal mutations (Fig. 6 A and Fig. S3 C). At higher magnification these organelles appeared as multivesicular bodies (MVBs; Fig. 6, B and C). MVBs are endosome-derived organelles containing 30–90 nm vesicles, which grow from early and recycling endosomes or from the trans-Golgi network and evolve into lysosomes or into secretory organelles (Raiborg et al., 2003). Hence, MVB accumulation may reflect either an endocytic/degradation pathway or a secretory defect. To distinguish between these two possibilities, we examined whether *vha-5* mutants had normal lysosomes. In addition, we compared *vha-5* defects to those induced by strong mutations in *vps-27*, *rme-8*, and *cup-5*, which are three essential genes acting at different steps along the endocytic route (Zhang et al., 2001; Treusch et al., 2004; Roudier et al., 2005). The rationale for this comparison is that if *vha-5* cuticle mutations affect endocytosis,

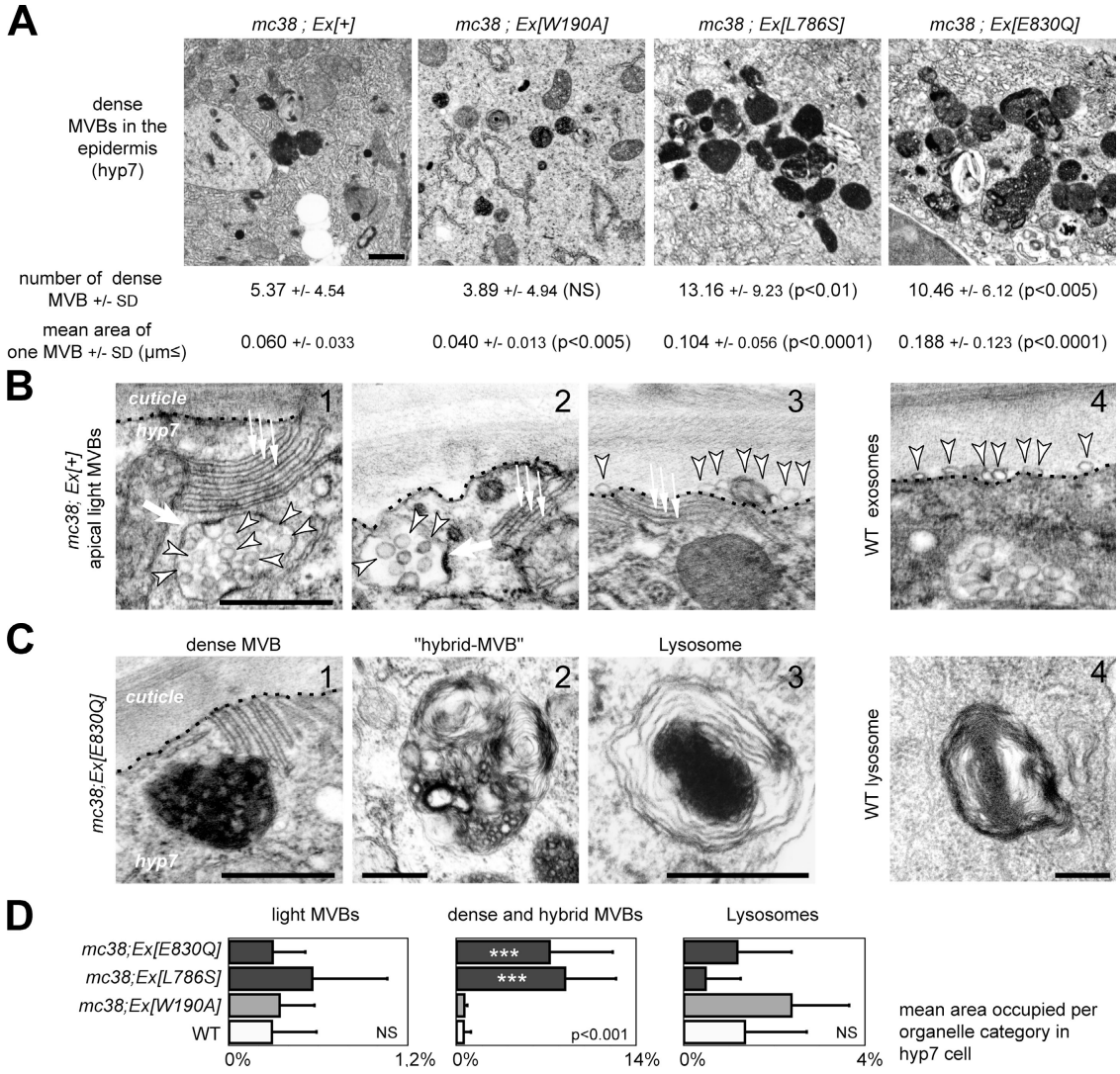

Figure 6. **Cuticle mutations impair MVB-driven exosome release.** TEM micrographs of the adult epidermis. (A) Dense MVBs at low magnification (genotypes indicated above images); the number and size of MVBs are quantified below images. Note that L786S and E830Q mutations increase MVB size and number. (B) Light MVBs at higher magnification in control *mc38; Ex[+]* (B1–B3) and wild-type (B4) adults. Note MVB organelles (thick arrows) with intralumenal vesicles (arrowheads), in direct apposition to membrane stacks (thin arrows) at the apical epidermal plasma membrane (B1), or in apparent fusion with the plasma membrane (B2). The presence of vesicles externally (B3 and B4) suggests that these MVBs are secretory and that intralumenal vesicles become exosomes. (C) MVBs and lysosomes in *mc38; Ex[E830Q]* (C1–C3) and wild-type (C4) adults. MVBs are electron dense (C1), yet can evolve into normal lysosomes (C2 and C3, compare to C4). Bars, 0.5 µm. (D) Quantification of endocytic organelles in *vha-5* mutants (error bars represent the SD; ***, significantly different from wild type; $P < 0.0001$). Cuticle mutants specifically accumulate dense and hybrid MVBs.

then *vps-27*, *rme-8*, or *cup-5* mutations should induce cuticle phenotypes comparable to those of *vha-5* mutants. As found in other systems (Luzio et al., 2001), we could observe in all *vha-5* mutants intermediate late endosome–lysosome compartments corresponding to enlarged MVBs with multilamellar structures (called hybrid-MVBs in the next section) and normal lysosomes, suggesting that the endocytic/degradation pathway was not qualitatively affected (Fig. 6 C). In contrast, *cup-5(ar465)* mutants accumulated large MVBs in their epidermis that did not evolve into lamellar structures (Fig. 7 A). Furthermore, *vps-27(ok579)*, *rme-8(b1023)*, and *cup-5(ar465)* mutants had normal alae, unlike *vha-5* cuticle mutants (Fig. 7, B and C). We conclude that cuticle mutations are unlikely to affect degradation, and, rather, they affect a secretory pathway.

To understand the relevance of MVB accumulation in *vha-5* mutants, we reinvestigated secretion in the wild-type *C. elegans* epidermis. In hematopoietic cells, some MVBs release their vesicle content into the extracellular space and, thus, play a role in exocytosis, in addition to their well defined role in the endosomal pathway (de Gassart et al., 2004). The vesicles released by fusion of MVBs with the plasma membrane were originally called exosomes in antigen-presenting cells. In support of the notion that secretion in the *C. elegans* epidermis involves exosomes, we observed small light MVBs containing 50–100-nm vesicles just beneath the apical plasma membrane. Moreover, we occasionally saw vesicles immediately above the plasma membrane in the inner cuticular layer, strongly suggesting that a MVB had released its intralumenal vesicles (Fig. 6 B). These MVBs were always found in the vicinity of epidermal apical membrane stacks, a structure whose role is so far unknown (White, 1988). In contrast, we rarely observed similar MVBs adjacent to the plasma membrane in cuticle mutants, or they were darker (Fig. 6 C). These data suggest that the MVB-limiting membrane can fuse with the apical membrane to release exosomes in the cuticle, and show that this process is impaired in *vha-5* cuticle mutants. It raises the possibility that the V0 sector is critical for MVB fusion with the apical membrane during exosome release.

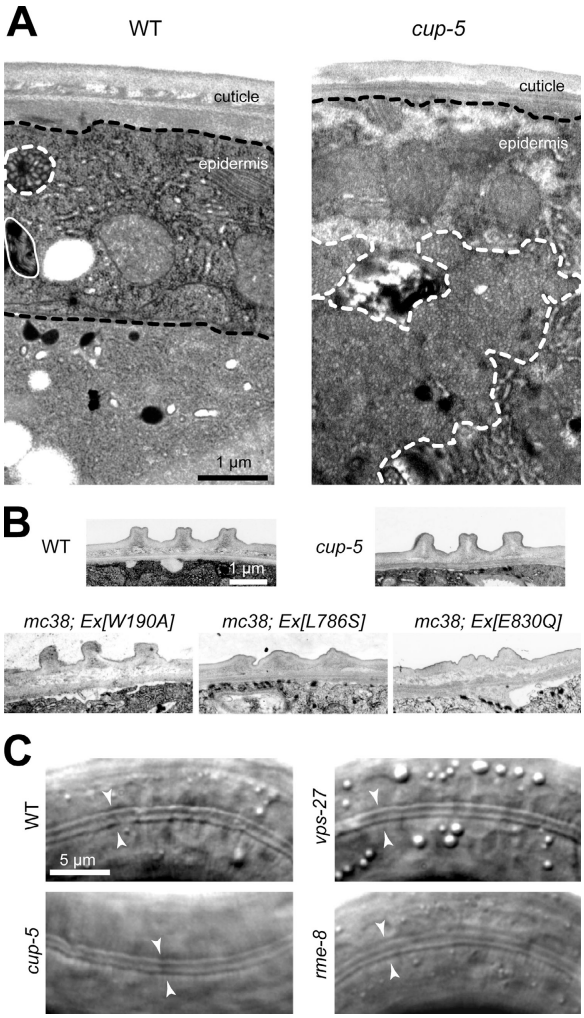

Figure 7. **Fluid-phase endocytosis mutations do not affect cuticle formation.** (A) Epidermis of a *cup-5(ar465)* adult visualized by TEM; note the enlarged electron-dense MVB (demarcated by dotted lines). (B) Adult alae visualized by TEM (genotypes are indicated on the left). (C) Alae of L1 larvae grown at 25°C and visualized by DIC; *vps-27(ok579)* is an L2 lethal mutation and *rme-8(b1023)* is a temperature-sensitive lethal mutation. *vps-27*, *rme-8*, and *cup-5* mutations did not affect alae formation, in contrast to *vha-5* cuticle mutations.

V0 mediates secretion of hedgehog-like peptides

An important expectation of the cuticle defects described so far is that we should be able to identify cuticular proteins whose secretion depends on VHA-5 activity. Cuticle proteins include collagens and Hedgehog-related peptides (McMahon et al., 2003; Zugasti et al., 2005). We found that the collagen DPY-7 was efficiently secreted in *vha-5(mc38)*–null animals, in animals carrying cuticle mutations, as well as in *che-14(mc35)* mutants (Fig. S4, available at http://www.jcb.org/cgi/content/full/jcb.200511072/DC1). We turned our attention onto Hedgehog-related peptides, which appeared as good candidates for three reasons. First, *vha-5* alae defects partially resemble those observed in *che-14* mutants. Second, CHE-14 is homologous to Dispatched, which is a protein required for Hedgehog release (Burke et al., 1999; Michaux et al., 2000). Third, despite the absence of a Hedgehog homologue in *C. elegans*, its genome contains several Hedgehog-related peptides required to generate a normal cuticle, although their precise roles remain unknown (Aspock et al., 1999; Zugasti et al., 2005).

We tagged with GFP the secreted domain of the Hedgehog-related peptides WRT-2 and -8 (Fig. 8 A and Fig. S3 E), which are expressed in the epidermis (Aspock et al., 1999). We found that animals bearing cuticle mutations, but not canal mutations, accumulated VHA-5::RFP and WRT-2::GFP or -8::GFP in discrete entities in their epidermis (Fig. 8, B and C; and Fig. S3, D and F). These entities most likely correspond to the dense and hybrid MVBs (Fig. 6, C and D) because VHA-5::RFP also colocalized (Fig. 8 C) with the MVB marker VPS-27::GFP (Roudier et al., 2005). Moreover, both VHA-5 antiserum and a GFP antiserum targeting WRT-2::GFP decorated the MVBs of cuticle mutants (Fig. 8 D and Fig. S5 B, available at http://www.jcb.org/cgi/content/full/jcb.200511072/DC1). Last, in wild-type nontransgenic animals, in addition to membrane stacks (Fig. 1 G), VHA-5 was found at the MVB-limiting membrane, in

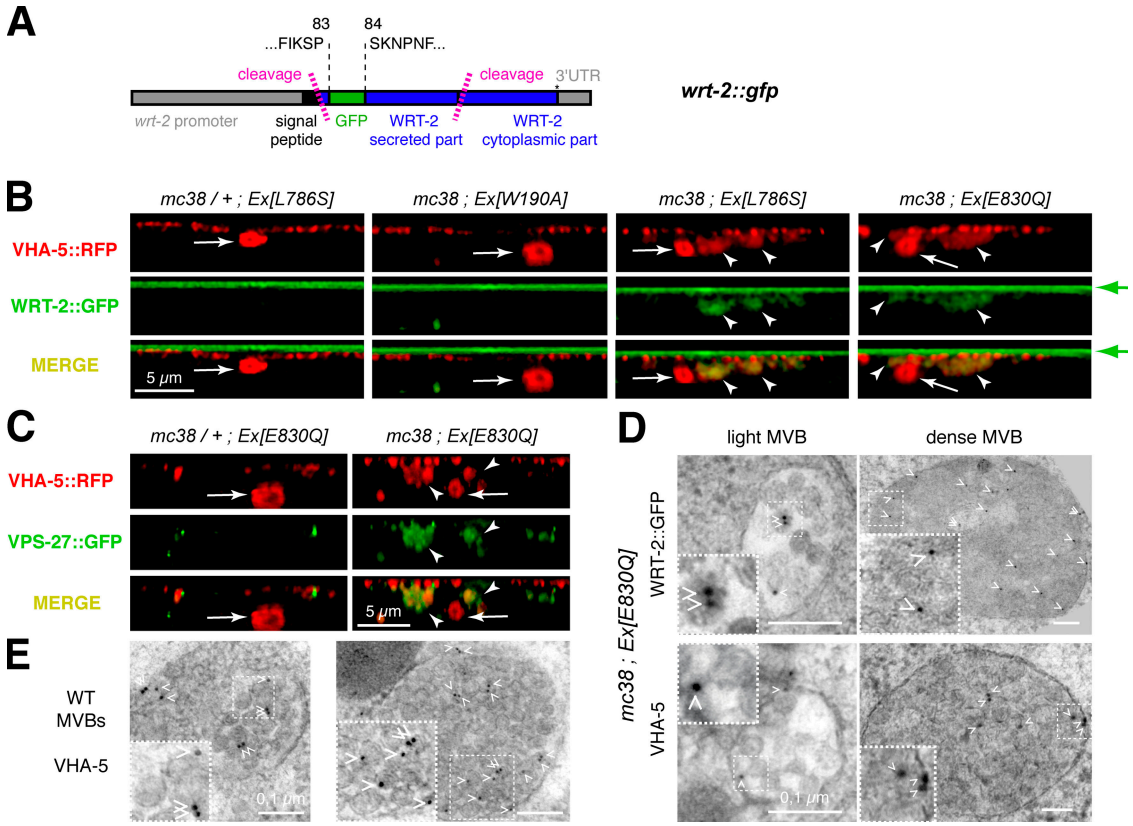

Figure 8. **The V0 sector is required for the secretion of Hedgehog-related peptides through MVBs.** (A) Structure of the *wrt-2::gfp* construct. GFP was inserted in frame in a nonconserved region after the signal peptide cleavage site, rather than at the COOH terminus because the related WRT-1 protein undergoes autoprocessing in vitro, like Hedgehog (Porter et al., 1996). (B) XZ projections of serial confocal sections through the epidermis of adults expressing mutant VHA-5::mRFP and WRT-2::GFP constructs (white arrowheads, VHA-5 and WRT-2 in the epidermis; white arrows, excretory canal; part of the green signal was caused by autofluorescence, arrow on the right). The L786S mutation induced coretention of VHA-5::mRFP and WRT-2::GFP in homozygous (third set of images), but not in heterozygous (first set of images), *vha-5(mc38)* animals. The mixed mutation W327A, and the cuticle mutations L786S and V844F resulted in similar coretention phenotypes (Fig. S3 D and not depicted). (C) XZ projections of serial confocal sections through the epidermis of *mc38; Ex[E830Q]* adults expressing the MVB marker VPS-27::GFP construct. (D and E) Immunogold localization of VHA-5 (D and E) and WRT-2::GFP (D) in MVBs of *mc38; Ex[E830Q]* mutant (two different samples; D) and wild-type adults (E). Fig. S3 is available at http://www.jcb.org/cgi/content/full/jcb.200511072/DC1.

intralumenal vesicles, and in the cuticle (Fig. 8 E and Fig. S5 A), suggesting that it could act at different steps in the secretion of vesicle (see Discussion). Importantly, the VHA-5 protein with the substitutions L786S (Fig. 8 B) or E830Q (not depicted) could reach the plasma membrane in heterozygous *vha-5(mc38)/+* animals, which strongly suggests that their intracellular retention in homozygous *mc38* animals is caused by the loss of a trafficking function rather than by misfolding. Consistently, the WRT-2/8 proteins were not retained intracellularly either in heterozygous *vha-5(mc38)/+* animals, despite the presence of the L786S (Fig. 8 B), or in E830Q transgenes (not depicted). These results indicate that the V0 sector plays a key role in a specific apical secretion pathway that is taken on by Hedgehog-related proteins, but not by collagens.

Discussion

Whereas basolateral secretion is known to depend on the activity of specific complexes (AP-1B and the exocyst), no such complex has been implicated in apical secretion. In addition, although recycling endosomes appear to play a central role in basolateral secretion, their importance in apical secretion is still under active investigation. Our characterization of mutations affecting the V-ATPase "a" subunit VHA-5 sheds new light on the apical biosynthetic secretory pathway. We could observe the fusion of MVBs with the apical plasma membrane in wild-type animals, and the subsequent release of exosomes. In contrast, we found that some VHA-5 mutations accumulate MVBs in their epidermis and prevent the secretion of Hedgehog-related proteins. Thus, we propose a model whereby apical secretion of Hedgehog-related proteins involves their incorporation into the intralumenal vesicles of MVBs, and their subsequent release when MVBs fuse with the apical plasma membrane (Fig. 9). Furthermore, we suggest that the V0 sector of the V-ATPase plays a key role in this process.

We can envision two scenarios for the role of the V0 sector. First, *vha-5* mutations affecting cuticle formation could decrease V-ATPase proton pumping along the biosynthetic secretory route to indirectly impair secretion. Consistent with this possibility, mutations in *S. cerevisiae* Vph1p (L746S, E789Q, and V803F) corresponding to the cuticle mutations (L786S, E830Q, and V844F, respectively) strongly reduce, but do not

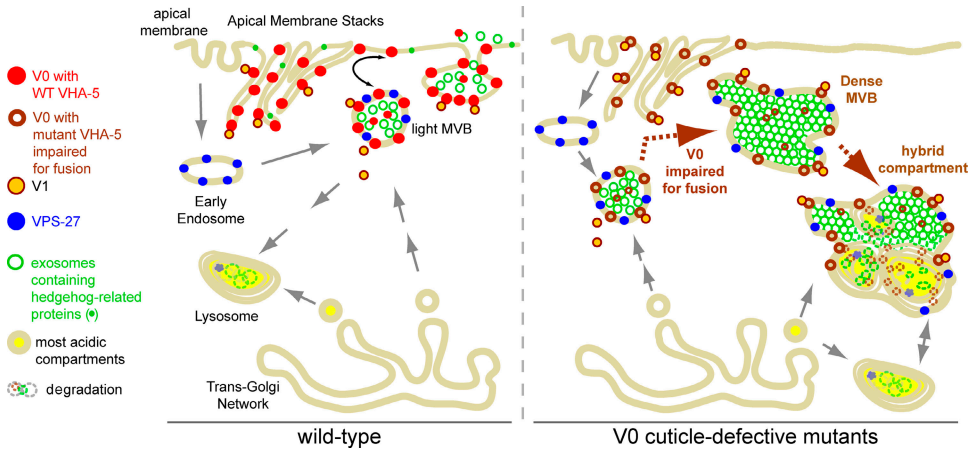

Figure 9. **Model for apical secretion mediated by the V0 sector of the V-ATPase.** We propose that in a wild-type animal (left) the V0 sector mediates fusion between the limiting membrane of MVBs and the apical plasma membrane (curved double-headed arrow). This model is supported by our genetic data, by the presence of VHA-5 at the apical plasma membrane (Fig. 1, E–G) and the MVB-limiting membrane (Fig. 8 E and Fig. S5 A), and by the accumulation of dense or hybrid MVBs in cuticle mutants (Fig. 8, Fig. S3 D, and Fig. S5, B–D). We expect the existence of two distinct V0 populations, some mediating secretion, others mediating proton pumping with the V1 sector. In cuticle defective *vha-5* mutants (right), most fusion events between MVBs and the plasma membrane are compromised so that MVBs grow and become denser by accumulating their content, which can nevertheless be normally degraded.

eliminate, proton pumping (Leng et al., 1996, 1998). We think, however, that this possibility is unlikely because in yeast proton uptake is not limiting for fusion of Vph1p-defective vacuoles (Bayer et al., 2003). Alternatively, these mutations could uncover a direct role of the V0 sector in apical exocytosis, independently of the V1 sector. Four observations strongly support this notion. First, inhibition of V1 subunits did not affect cuticle formation, although it strongly impaired osmoregulation and endocytosis. Second, we obtained specific V0 mutations inducing a strong cuticular phenotype without any apparent pumping-related defect in the excretory cell. Third, these mutations selectively affected the secretion of Hedgehog-related proteins, but not collagens. Last, strong mutations in well characterized genes blocking different steps of fluid-phase endocytosis did not affect cuticle structure. The specific accumulation of dense and hybrid MVBs, but not of light MVBs, in cuticle mutants, as well as the detection of significant amounts of WRT-2::GFP within these MVBs, suggests that VHA-5 is neither required to form MVBs nor to load them with cargo proteins. Instead, the presence of VHA-5 at the MVB-limiting and apical membranes suggests that the V0 sector could drive the fusion of MVBs with the apical membrane via the formation of V0 sectors transcomplexes between both membranes (Fig. 9), as suggested in yeast vacuole fusion and at the *D. melanogaster* synapse (Bayer et al., 2003; Hiesinger et al., 2005; Peters et al., 2001). In vertebrates, 300-nm procollagen-I rod bundles assemble in the ER and travel through the Golgi lumen (Bonfanti et al., 1998). Assuming that worm collagens are secreted this way, they would not fit into exosomes, suggesting that there are at least two distinct secretion pathways in the epidermis, one involving the V0 sector and another followed by collagens.

What could explain a common requirement for the V0 sector during the *C. elegans* apical exocytosis, yeast vacuole fusion, and *D. melanogaster* synaptic transmission? The prevailing view is that a SNAREpin complex initiates membrane fusion once a vesicle has been docked to a proper membrane (Chernomordik and Kozlov, 2003; Jahn et al., 2003). Although the V0 sector is thought to act downstream of SNAREs in yeast and *D. melanogaster* (Peters et al., 2001; Bayer et al., 2003; Hiesinger et al., 2005), we cannot exclude that it also acts in parallel to SNAREs, at least in *C. elegans*, to dock MVBs. Another possibility is that V0 transcomplexes initiate the formation of a protein pore, as initially suggested in yeast (Peters et al., 2001). On the other hand, expansion of the fusion pore is considered as the limiting step in membrane fusion, and might require additional catalysts in vivo (Chernomordik and Kozlov, 2003). Such a role could be fulfilled by the V0 sector, either to overcome constraints caused by the big size and/or the specific lipoproteic content of *C. elegans* epidermal MVBs and yeast vacuoles, or to allow rapid synaptic transmission in *D. melanogaster* neurons (Hiesinger et al., 2005).

Irrespective of the precise role of the V0 sector in membrane fusion, our findings bear potentially important implications. First, morphogens such as Wingless and Hedgehog in *D. melanogaster*, or Sonic-Hedgehog at the mouse node, might be secreted through a similar pathway because their secretion involves particles possibly related to exosomes (Greco et al., 2001; Gallet et al., 2003; Panakova et al., 2005; Tanaka et al., 2005). A major objective will be to determine whether CHE-14 and Dispatched act in the aforementioned secretory pathway, and, if so, at which step. Second, several other cell types, such as antigen-presenting cells, reticulocytes, and some epithelial cells, can release exosomes (de Gassart et al., 2004), which might thus also require the V0 sector for their secretion. In particular, the V0 sector might be directly associated with the transmission of some infectious diseases because viruses, such as HIV and the prion protein, can be disseminated through MVBs and the exosome-releasing machinery (de Gassart et al., 2004; Fevrier et al., 2005). Likewise, the aforementioned secretory pathway could be involved in innate immunity because expression of the Hedgehog-related peptide GRD-3 is induced in *C. elegans* upon bacterial infection (Couillault et al., 2004).

Third, our findings raise the issue of the origin of the MVBs. Interestingly, the apical recycling endosomes have been recognized to play an important role in biosynthetic secretory pathways (Hoekstra et al., 2004). Future studies should reveal whether the secretory MVBs that we described could originate from this compartment.

In conclusion, our work shows that trafficking to the apical membrane of at least some lipid-modified proteins involves specific protein complexes (the V-ATPase V0 sector), much as trafficking to the basolateral membrane, and predicts a key role for MVBs in apical exocytosis.

Materials and methods

Strain maintenance and RNA interference

Worms were grown at 20°C (unless noted otherwise; Brenner, 1974). The identification of *mc37* and *mc38* as *vha-5/F35H10.4*-null mutations will be described elsewhere (the gene affected by *mc37* and *mc38* was initially named *rdy-1*; see www.wormbase.org). Marker and alleles used were as follows: *cup-5(ar465)* (Treusch et al., 2004), *rme-8(b1023ts), bls1[vit-2::gfp; rol-6(su1006)]* (Zhang et al., 2001), and *vps-27(ok579)/unc-24(e138) dpy-20(e1282)* (Roudier et al., 2005). The L1 alae phenotype of *rme-8(b1023ts)* was scored by allowing adults to lay eggs for 1 h at 15°C, and then transferring embryos to 25°C after egg laying. RNAi was performed using the following bacterial clones from the Wellcome–Medical Research Council library (Kamath et al., 2003): *vha-1*, III-5A20; *vha-4*, II-5J16; *vha-5*, IV-4O13; *vha-8*, IV-3I08; and *vha-13*, V-9O06 (www.wormbase.org). To score L1 larvae, RNAi was induced in L4 larvae; to score adults, RNAi was induced in larvae at the L2–L3 molt. Feeding plasmids were retransformed into fresh HT115 (DE3) bacteria, selecting for tetracycline and ampicillin resistance.

Plasmids

Cloning of the *vha-5* coding sequence with a 2.8-kb promoter upstream of the GFP coding sequence in the pPD95.75 vector (Fire kit) generated a rescuing *vha-5::gfp* construct. A *vha-5::mrfp* construct was obtained by replacing the GFP with the monomeric red fluorescent protein (mRFP) coding sequence in the *vha-5::gfp* construct. A *vha-8::yfp* construct was obtained by cloning the *vha-8* coding sequence and a 3-kb promoter upstream of the YFP coding sequence in the pPD136.64 vector (Fire kit). To generate *wrt-2::gfp* and *wrt-8::gfp* constructs, we cloned *wrt-2* and *-8* genomic DNA with their 5′ and 3′ regulatory sequences into pBSKII-derived plasmids. The GFP coding sequence was inserted in a nonconserved region of the predicted secreted peptide (Fig. 8 A and Fig. S3 D).

Site-directed mutagenesis of VHA-5::GFP

The *vha-5::gfp* construct was mutated using the QuikChange Site-Directed Mutagenesis kit (Stratagene). Each desired mutation, and the entire *vha-5* coding sequence of most important plasmids, was verified. Mutant plasmids were microinjected in heterozygous *vha-5(mc38)/unc-5(e53)* at 3 ng/µl, along with the marker pRF4 *[rol-6(su1006)]* at 100 ng/µl, *wrt-2::gfp* or *wrt-8::gfp* constructs at 30 ng/µl (when relevant), and pBSKII plasmid at up to 200 ng/µl. Absence of *unc-5* animals in the progeny was used as a criterion for rescue. mRFP versions for the mutations W190A, R191A, W327A, L786S, E830Q, and V844F were obtained from GFP derivatives without PCR amplification and resulted in similar phenotypes. At least two independent extrachromosomal lines were initially examined for each mutation. More detailed analysis was performed on a representative line.

VHA-5 antiserum, Western blots, and immunofluorescence

VHA-5 polyclonal antibodies were raised in rabbits injected with a purified GST fusion protein containing VHA-5 residues I29–M302, which was obtained by cloning a fragment amplified from the cDNA *yk458f4* (a gift from Y. Kohara, National Institute of Genetics, Mishima, Japan) into the vector pGEX-2T. Total worm extracts were solubilized in 8 M urea/2% SDS by sonication, before 8% acrylamide gel electrophoresis and Western blotting. VHA-5 antiserum was used at 1:2,000, the actin monoclonal antibody (act-2D7; Institut de Génétique et de Biologie Moléculaire et Cellulaire collection) at 1:4,000; primary antibodies were revealed with a SuperSignal kit (Pierce Chemical Co.). Immunofluorescence was performed using the VHA-5 antiserum at 1:1,000 dilution and the DPY-7 monoclonal antibody (gift from I. Johnstone, Wellcome Centre for Molecular Parasitology, Glasgow, Scotland) at a 1:50 dilution.

DIC and confocal microscopy

Animals were mounted on 4% agarose pads in M9, anaesthetized with 0.2% tricaine/0.02% tetramisole in M9. For DIC imaging, we used a microscope (Axioplan; Carl Zeiss MicroImaging, Inc.) coupled to a camera (CoolSNAP; Roper Scientific) under a 100× objective (PlanApo; Leica). For Fig. 4 A, we took at least 40 pictures of adult worms per strain and used ImageJ (National Institutes of Health) to measure the distance between the rectum and the grinder. Confocal images were captured on a confocal microscope (SP2-AOBS; Leica), scanning every 122 nm for XZ sections through a 100× objective with a 2.15× zoom (Fig. 8, B and C; and Fig. S3 D) or a 4× zoom (Fig. 4 E and Fig. 5). Images were processed with the Tcstk software (McMahon et al., 2001) and edited using Photoshop 7.0 (Adobe). Microscopes were in an air-conditioned room (20–21°C).

TEM and SEM

L4 larvae were transferred onto fresh plates for 24 ± 2 h at 20°C before fixation. For TEM, but not for SEM, animals were sectioned and fixed for at least 24 h in 2.5% glutaraldehyde/2% paraformaldehyde/0.1 M sodium cacodylate, pH 7.2, at 4°C, and then postfixed for 5 h with 2% osmium tetroxide in the same buffer at 4°C, dehydrated in graded alcohol/water mixes, and embedded in Epon. Ultrathin 70-nm sections were contrasted with uranyl acetate and lead citrate. Sections were observed with a microscope (CM12; Philips) operating at 60 kV. Quantification of the excretory canal section area was obtained using the Metamorph software after scanning images were captured at a 17,000× magnification. Quantification of MVBs was performed on 3,600×-magnified images. Quantification of the mean area occupied by organelles (Fig. 6 D) was obtained using ImageJ and dividing the total surface of each organelle subtype by the cytoplasmic surface of the hyp7 epidermis section. At least four animals per mutant strain were examined, and more than nine pictures per animal from different ultrathin sections were analyzed. For SEM, animals were postfixed for 1 h with 2% osmium tetroxide at 4°C, dehydrated, and critical point dried in hexamethyldisilazane. Fixed animals were mounted on stubs, coated with palladium, and observed through a microscope (XL20; Philips). At least 20 animals per strain were analyzed.

High pressure freezing and immunogold labeling

Adult worms were frozen with a high pressure freezing apparatus (EMPACT-2; Leica) in 20% BSA/M9 medium. Cryosubstitution was conducted as in Muller-Reichert et al. (2003). Ultrathin sections were collected on formvar-carbon–coated copper grids and processed for immunogold labeling. Blocking was performed in PBS/glycine 150 mM, and then in PBS/1% BSA/0.1% Cold Water Fish Skin Gelatin (CWFSG; Aurion) for 30 min. Rabbit anti–VHA-5 at 1:1,000 and rabbit anti-GFP at 1:500 (ab6556; AbCam) were incubated for 1 h in PBS/0.1% CWFSG. 10 nm protein A–coupled gold beads (1:50; University Medical Center, Utrecht, Netherlands) were incubated for 1 h in PBS/0.1% CWFSG. Postfixation was achieved in 2.5% glutaraldehyde, contrasted by uranyl acetate/lead citrate. Images were acquired at 60 kV on a microscope (Morgagni; FEI) with a charge-coupled device camera (Megaview III; Soft Imaging System).

Online supplemental material

Fig. S1 provides a control for Fig. 2 B, showing that RNAi against *vha-5* was efficient. In addition, it presents the yolk endocytosis defects induced by the loss of V-ATPase activity (yolk proteins are produced by the intestine and are essential for embryonic development); it suggests that RNAi treatment against V0 and V1 subunits was equally effective, and contributes to establish that alae differences described in Fig. 2 are meaningful. Fig. S2 summarizes the main phenotypes observed in *vha-5(mc38)* animals carrying transgenes with the mutations shown in Fig. 3. Fig. S3 presents the excretory canal, cuticle and MVB phenotypes induced by the mutations R191A, W327A and V844A, which are discussed but not illustrated in the main text, and shows that WRT-8::GFP accumulates in *mc38; Ex[vha-5(E830Q)::rfp]* animals; it should be viewed along with Figs. 4, 6 and 8. Fig. S4 shows that secretion of the collagen DPY-7 is not affected by *vha-5* or *che-14* mutations. Fig. S5 provides larger pictures and controls for the immunogold experiments shown in Fig. 8. Online supplemental material is available at http://www.jcb.org/cgi/content/full/jcb.200511072/DC1.

We are grateful to Guillaume Belliard, Grégoire Michaux, and Emmanuel Sotirakis for their help in isolating *vha-5* mutations, and to Satis Sookhareea for expert assistance in producing VHA-5 antiserum. We thank the Institut de Génétique et de Biologie Moléculaire et Cellulaire Imaging Facility for help with

confocal and EM, and Patrick Schultz for access to the EMPACT2. We thank Andy Fire, Yuji Kohara, Johnny Fares, Barth Grant, Iain Johnstone, Renaud Legouis, and the CGC for reagents. We thank Jean-Louis Bessereau, Thierry Galli, Pierre Gönczy, Nathalie Pujol, and Christelle Gally for critical reading of the manuscript.

S. Liégeois and A. Benedetto were supported by fellowships from the Ministère de la Recherche, and from the FRM. This work was supported by funds from the Centre National de la Recherche Scientifique, Institut National de la Santé et de la Recherche Médicale, and by a grant from the Ministère de la Recherche (programme ACI).

Submitted: 17 November 2005
Accepted: 15 May 2006

References

Amara, S.G., and M.J. Kuhar. 1993. Neurotransmitter transporters: recent progress. *Annu. Rev. Neurosci.* 16:73–93.

Ang, A.L., T. Taguchi, S. Francis, H. Folsch, L.J. Murrells, M. Pypaert, G. Warren, and I. Mellman. 2004. Recycling endosomes can serve as intermediates during transport from the Golgi to the plasma membrane of MDCK cells. *J. Cell Biol.* 167:531–543.

Aspock, G., H. Kagoshima, G. Niklaus, and T.R. Burglin. 1999. *Caenorhabditis elegans* has scores of hedgehog-related genes: sequence and expression analysis. *Genome Res.* 9:909–923.

Bayer, M.J., C. Reese, S. Buhler, C. Peters, and A. Mayer. 2003. Vacuole membrane fusion: V0 functions after trans-SNARE pairing and is coupled to the Ca2+-releasing channel. *J. Cell Biol.* 162:211–222.

Beronja, S., P. Laprise, O. Papoulas, M. Pellikka, J. Sisson, and U. Tepass. 2005. Essential function of *Drosophila* Sec6 in apical exocytosis of epithelial photoreceptor cells. *J. Cell Biol.* 169:635–646.

Blott, E.J., and G.M. Griffiths. 2002. Secretory lysosomes. *Nat. Rev. Mol. Cell Biol.* 3:122–131.

Bonfanti, L., A.A. Mironov Jr., J.A. Martinez-Menarguez, O. Martella, A. Fusella, M. Baldassarre, R. Buccione, H.J. Geuze, A.A. Mironov, and A. Luini. 1998. Procollagen traverses the Golgi stack without leaving the lumen of cisternae: evidence for cisternal maturation. *Cell*. 95:993–1003.

Bonifacino, J.S., and J. Lippincott-Schwartz. 2003. Coat proteins: shaping membrane transport. *Nat. Rev. Mol. Cell Biol.* 4:409–414.

Brenner, S. 1974. The genetics of *Caenorhabditis elegans. Genetics*. 77:71–94.

Burke, R., D. Nellen, M. Bellotto, E. Hafen, K.A. Senti, B.J. Dickson, and K. Basler. 1999. Dispatched, a novel sterol-sensing domain protein dedicated to the release of cholesterol-modified hedgehog from signaling cells. *Cell*. 99:803–815.

Cheong, K.H., D. Zacchetti, E.E. Schneeberger, and K. Simons. 1999. VIP17/MAL, a lipid raft-associated protein, is involved in apical transport in MDCK cells. *Proc. Natl. Acad. Sci. USA*. 96:6241–6248.

Chernomordik, L.V., and M.M. Kozlov. 2003. Protein-lipid interplay in fusion and fission of biological membranes. *Annu. Rev. Biochem.* 72:175–207.

Choi, K.Y., Y.J. Ji, B.K. Dhakal, J.R. Yu, C. Cho, W.K. Song, and J. Ahnn. 2003. Vacuolar-type H+-ATPase E subunit is required for embryogenesis and yolk transfer in *Caenorhabditis elegans. Gene*. 311:13–23.

Couillault, C., N. Pujol, J. Reboul, L. Sabatier, J.-F. Guichou, Y. Kohara, and J.J. Ewbank. 2004. TLR-independent control of innate immunity in *Caenorhabditis elegans* by the TIR domain adaptor protein TIR-1, an ortholog of human SARM. *Nat. Immunol.* 5:488–494.

de Gassart, A., C. Geminard, D. Hoekstra, and M. Vidal. 2004. Exosome secretion: the art of reutilizing nonrecycled proteins? *Traffic*. 5:896–903.

Fevrier, B., D. Vilette, H. Laude, and G. Raposo. 2005. Exosomes: a bubble ride for prions? *Traffic*. 6:10–17.

Fiedler, K., F. Lafont, R.G. Parton, and K. Simons. 1995. Annexin XIIIb: a novel epithelial specific annexin is implicated in vesicular traffic to the apical plasma membrane. *J. Cell Biol.* 128:1043–1053.

Folsch, H., H. Ohno, J.S. Bonifacino, and I. Mellman. 1999. A novel clathrin adaptor complex mediates basolateral targeting in polarized epithelial cells. *Cell*. 99:189–198.

Gallet, A., R. Rodriguez, L. Ruel, and P.P. Therond. 2003. Cholesterol modification of hedgehog is required for trafficking and movement, revealing an asymmetric cellular response to hedgehog. *Dev. Cell*. 4:191–204.

Grant, B., and D. Hirsh. 1999. Receptor-mediated endocytosis in the *Caenorhabditis elegans* oocyte. *Mol. Biol. Cell*. 10:4311–4326.

Greco, V., M. Hannus, and S. Eaton. 2001. Argosomes: a potential vehicle for the spread of morphogens through epithelia. *Cell*. 106:633–645.

Grindstaff, K.K., C. Yeaman, N. Anandasabapathy, S.C. Hsu, E. Rodriguez-Boulan, R.H. Scheller, and W.J. Nelson. 1998. Sec6/8 complex is recruited to cell-cell contacts and specifies transport vesicle delivery to the basal-lateral membrane in epithelial cells. *Cell*. 93:731–740.

Hiesinger, P.R., A. Fayyazuddin, S.Q. Mehta, T. Rosenmund, K.L. Schulze, R.G. Zhai, P. Verstreken, Y. Cao, Y. Zhou, J. Kunz, and H.J. Bellen. 2005. The v-ATPase V0 subunit a1 is required for a late step in synaptic vesicle exocytosis in *Drosophila. Cell*. 121:607–620.

Hoekstra, D., D. Tyteca, and S.C. van Ijzendoorn. 2004. The subapical compartment: a traffic center in membrane polarity development. *J. Cell Sci.* 117:2183–2192.

Hua, W., D. Sheff, D. Toomre, and I. Mellman. 2006. Vectorial insertion of apical and basolateral membrane proteins in polarized epithelial cells revealed by quantitative 3D live cell imaging. *J. Cell Biol.* 172:1035–1044.

Jahn, R., T. Lang, and T.C. Sudhof. 2003. Membrane fusion. *Cell*. 112:519–533.

Kamath, R.S., A.G. Fraser, Y. Dong, G. Poulin, R. Durbin, M. Gotta, A. Kanapin, N. Le Bot, S. Moreno, M. Sohrmann, et al. 2003. Systematic functional analysis of the *Caenorhabditis elegans* genome using RNAi. *Nature*. 421:231–237.

Kawasaki-Nishi, S., T. Nishi, and M. Forgac. 2001. Yeast V-ATPase complexes containing different isoforms of the 100-kDa a-subunit differ in coupling efficiency and in vivo dissociation. *J. Biol. Chem.* 276:17941–17948.

Kurzchalia, T.V., P. Dupree, R.G. Parton, R. Kellner, H. Virta, M. Lehnert, and K. Simons. 1992. VIP21, a 21-kD membrane protein is an integral component of trans-Golgi-network-derived transport vesicles. *J. Cell Biol.* 118:1003–1014.

Langevin, J., M.J. Morgan, J.B. Sibarita, S. Aresta, M. Murthy, T. Schwarz, J. Camonis, and Y. Bellaiche. 2005. *Drosophila* exocyst components Sec5, Sec6, and Sec15 regulate DE-cadherin trafficking from recycling endosomes to the plasma membrane. *Dev. Cell*. 9:355–376.

Leng, X.H., M.F. Manolson, Q. Liu, and M. Forgac. 1996. Site-directed mutagenesis of the 100-kDa subunit (Vph1p) of the yeast vacuolar (H+)-ATPase. *J. Biol. Chem.* 271:22487–22493.

Leng, X.H., M.F. Manolson, and M. Forgac. 1998. Function of the COOH-terminal domain of Vph1p in activity and assembly of the yeast V-ATPase. *J. Biol. Chem.* 273:6717–6723.

Lock, J.G., and J.L. Stow. 2005. Rab11 in recycling endosomes regulates the sorting and basolateral transport of E-cadherin. *Mol. Biol. Cell*. 16:1744–1755.

Luzio, J.P., B.M. Mullock, P.R. Pryor, M.R. Lindsay, D.E. James, and R.C. Piper. 2001. Relationship between endosomes and lysosomes. *Biochem. Soc. Trans.* 29:476–480.

Manninen, A., P. Verkade, S. Le Lay, J. Torkko, M. Kasper, M. Füllekrug, and K. Simons. 2005. Caveolin-1 is not essential for biosynthetic apical membrane transport. *Mol. Cell. Biol.* 25:10087–10096.

McMahon, L., R. Legouis, J.L. Vonesch, and M. Labouesse. 2001. Assembly of *C. elegans* apical junctions involves positioning and compaction by LET-413 and protein aggregation by the MAGUK protein DLG-1. *J. Cell Sci.* 114:2265–2277.

McMahon, L., J.M. Muriel, B. Roberts, M. Quinn, and I.L. Johnstone. 2003. Two sets of interacting collagens form functionally distinct substructures within a *Caenorhabditis elegans* extracellular matrix. *Mol. Biol. Cell*. 14:1366–1378.

Michaux, G., A. Gansmuller, C. Hindelang, and M. Labouesse. 2000. CHE-14, a protein with a sterol-sensing domain, is required for apical sorting in *C. elegans* ectodermal epithelial cells. *Curr. Biol.* 10:1098–1107.

Muller-Reichert, T., H. Hohenberg, E.T. O'Toole, and K. McDonald. 2003. Cryoimmobilization and three-dimensional visualization of C. elegans ultrastructure. *J. Microsc.* 212:71–80.

Nelson, F.K., and D.L. Riddle. 1984. Functional study of the *Caenorhabditis elegans* secretory-excretory system using laser microsurgery. *J. Exp. Zool.* 231:45–56.

Nishi, T., and M. Forgac. 2002. The vacuolar (H+)-ATPases–nature's most versatile proton pumps. *Nat. Rev. Mol. Cell Biol.* 3:94–103.

Nurrish, S.J. 2002. An overview of *C. elegans* trafficking mutants. *Traffic*. 3:2–10.

Oka, T., T. Toyomura, K. Honjo, Y. Wada, and M. Futai. 2001. Four subunit a isoforms of *Caenorhabditis elegans* vacuolar H+-ATPase. Cell-specific expression during development. *J. Biol. Chem.* 276:33079–33085.

Paladino, S., D. Sarnataro, R. Pillich, S. Tivodar, L. Nitsch, and C. Zurzolo. 2004. Protein oligomerization modulates raft partitioning and apical sorting of GPI-anchored proteins. *J. Cell Biol.* 167:699–709.

Paladino, S., T. Pocard, M.A. Catino, and C. Zurzolo. 2006. GPI-anchored proteins are directly targeted to the apical surface in fully polarized MDCK cells. *J. Cell Biol.* 172:1023–1034.

Panakova, D., H. Sprong, E. Marois, C. Thiele, and S. Eaton. 2005. Lipoprotein particles are required for Hedgehog and Wingless signalling. *Nature*. 435:58–65.

Peters, C., M.J. Bayer, S. Buhler, J.S. Andersen, M. Mann, and A. Mayer. 2001. Trans-complex formation by proteolipid channels in the terminal phase of membrane fusion. *Nature*. 409:581–588.

Porter, J.A., S.C. Ekker, W.J. Park, D.P. von Kessler, K.E. Young, C.H. Chen, Y. Ma, A.S. Woods, R.J. Cotter, E.V. Koonin, and P.A. Beachy. 1996. Hedgehog patterning activity: role of a lipophilic modification mediated by the carboxy-terminal autoprocessing domain. *Cell*. 86:21–34.

Puertollano, R., F. Martin-Belmonte, J. Millan, M.C. de Marco, J.P. Albar, L. Kremer, and M.A. Alonso. 1999. The MAL proteolipid is necessary for normal apical transport and accurate sorting of the influenza virus hemagglutinin in Madin-Darby canine kidney cells. *J. Cell Biol.* 145:141–151.

Pujol, N., C. Bonnerot, J.J. Ewbank, Y. Kohara, and D. Thierry-Mieg. 2001. The *Caenorhabditis elegans unc-32* gene encodes alternative forms of a vacuolar ATPase a subunit. *J. Biol. Chem.* 276:11913–11921.

Raiborg, C., T.E. Rusten, and H. Stenmark. 2003. Protein sorting into multivesicular endosomes. *Curr. Opin. Cell Biol.* 15:446–455.

Roberts, B., C. Clucas, and I.L. Johnstone. 2003. Loss of SEC-23 in *Caenorhabditis elegans* causes defects in oogenesis, morphogenesis, and extracellular matrix secretion. *Mol. Biol. Cell*. 14:4414–4426.

Rodriguez-Boulan, E., G. Kreitze, and A. Musch. 2005. Organization of vesicular trafficking in epithelia. *Nat. Rev. Mol. Cell Biol.* 6:233–247.

Roudier, N., C. Lefebvre, and R. Legouis. 2005. CeVPS-27 is an endosomal protein required for the molting and the endocytic trafficking of the low-density lipoprotein receptor-related protein 1 in *Caenorhabditis elegans. Traffic*. 6:695–705.

Sapio, M.R., M.A. Hilliard, M. Cermola, R. Favre, and P. Bazzicalupo. 2005. The Zona Pellucida domain containing proteins, CUT-1, CUT-3 and CUT-5, play essential roles in the development of the larval alae in *Caenorhabditis elegans. Dev. Biol.* 282:231–245.

Satoh, A.K., J.E. O'Tousa, K. Ozaki, and D.F. Ready. 2005. Rab11 mediates post-Golgi trafficking of rhodopsin to the photosensitive apical membrane of *Drosophila* photoreceptors. *Development*. 132:1487–1497.

Schuck, S., and K. Simons. 2004. Polarized sorting in epithelial cells: raft clustering and the biogenesis of the apical membrane. *J. Cell Sci.* 117:5955–5964.

Tanaka, Y., Y. Okada, and N. Hirokawa. 2005. FGF-induced vesicular release of Sonic hedgehog and retinoic acid in leftward nodal flow is critical for left-right determination. *Nature*. 435:172–177.

TerBush, D.R., and P. Novick. 1995. Sec6, Sec8, and Sec15 are components of a multisubunit complex which localizes to small bud tips in *Saccharomyces cerevisiae*. *J. Cell Biol.* 130:299–312.

Treusch, S., S. Knuth, S.A. Slaugenhaupt, E. Goldin, B.D. Grant, and H. Fares. 2004. *Caenorhabditis elegans* functional orthologue of human protein h-mucolipin-1 is required for lysosome biogenesis. *Proc. Natl. Acad. Sci. USA*. 101:4483–4488.

White, J. 1988. The anatomy. *In* The Nematode *Caenorhabditis elegans*. Monograph 17. W.B. Wood and the Community of *C. elegans* Researchers, editors. Cold Spring Harbor Laboratory Press, Cold Spring Harbor, NY. 81–122.

Whyte, J.R., and S. Munro. 2002. Vesicle tethering complexes in membrane traffic. *J. Cell Sci.* 115:2627–2637.

Yeaman, C., K.K. Grindstaff, J.R. Wright, and W.J. Nelson. 2001. Sec6/8 complexes on trans-Golgi network and plasma membrane regulate late stages of exocytosis in mammalian cells. *J. Cell Biol.* 155:593–604.

Zhang, Y., B. Grant, and D. Hirsh. 2001. RME-8, a conserved J-domain protein, is required for endocytosis in *Caenorhabditis elegans. Mol. Biol. Cell*. 12:2011–2021.

Zugasti, O., J. Rajan, and P.E. Kuwabara. 2005. The function and expansion of the Patched- and Hedgehog-related homologs in *C. elegans. Genome Res.* 15:1402–1410.